ISSN 1070-3632, Russian Journal of General Chemistry, 2015, Vol. 85, No. 10, pp. 2366–2373. © Pleiades Publishing, Ltd., 2015.

Synthesis and Molecular Structure of Moxifloxacin Drug with Metal Ions as a Model Drug Against Some Kinds of Bacteria and Fungi[1]

S. M. El-Megharbel[a,b], A. M. A. Adam[a], A. S. Megahed[a], and M. S. Refat[a,c]

[a] *Department of Chemistry, Faculty of Science, Taif University, Al-Hawiah, Taif, P.O. Box 888, 21974 Saudi Arabia*

[b] *Department of Chemistry, Faculty of Science, Zagazig University, Zagazig, Egypt*

[c] *Department of Chemistry, Faculty of Science, Port Said University, Port Said, Egypt*
e-mail: samyelmegharbel@yahoo.com; msrefat@yahoo.com

Received May 9, 2015

Abstract—Metal complexes of antibiotic molecules can be used as antimicrobial mimetic drug models. The current study is devoted to the synthesis, physicochemical properties, computational, and antimicrobial activity of the products of chelation of moxifloxacin hydrochloride (mox-HCl) antibiotic drug and metal ions including Ca(II), Mg(II), Zn(II), and Fe(III). Structures of the complexes were elucidated on the basis of elemental analyses, electronic, IR, Raman, and ^{1}H NMR spectra. The data revealed that chelation of moxifloxacin could follow mono and bidentate pathways. Ca(II), Zn(II) and Fe(III) ions coordinated via N atoms of the piperidyl ring but Mg(II) coordinated via oxygen atoms of the carbonyl (quinolone) and carboxylic groups. According to molar conductance data the complexes had non-electrolyte nature. Formulas of the complexes can be presented as $[Mg(mox\text{-}HCl)_2(Cl)_2]\cdot 2H_2O$ (**1**), $[Ca(mox\text{-}HCl)_2(Cl)_2]\cdot 2H_2O$ (**2**), $[Zn(mox\text{-}HCl)_2(NO_3)_2]$ (**3**), and $[Fe(mox\text{-}HCl)_3(Cl)_3]$ (**4**). All synthesized mox-HCl complexes demonstrated some antibacterial but no antifungal activities.

Keywords: moxifloxacin hydrochloride, metal ions, chelation, spectroscopy, antimicrobial, nano-scale

DOI: 10.1134/S1070363215100230

INTRODUCTION

Moxifloxacin hydrochloride (mox-HCl, Fig. 1) is one of the fluoroquinolones that belongs to the 4th generation of drugs [1, 2].

Metal ions upon complexation with various antibiotic drugs can enhance antimicrobial activity of the latter ones [3–8]. Quinolones interact with the enzyme-DNA complex forming a drug-enzyme-DNA complex that blocks progression and the replication processes [9–12]. Quinolones can form mono and bidentate complexes with metals ions [13, 14]. Quinolones coordinate in a bidentate manner via one of oxygen atoms of the deprotonated carboxylic group and the ring carbonyl oxygen. Rarely, quinolones can act as bidentate ligand coordinating via two carboxyl oxygen atoms or both piperazine nitrogen atoms [13, 14] or as a unidentate ligand coordinated to metal ions via the terminal piperazinyl nitrogen [15]. The higher stoichiometry (1 : 4) was determined for complexes of quinolones with Bi^{3+} [16–18]. Some other studies devoted to complexation between quinolone drugs and metal ions should be mensioned here [19–24]. Coordination of fluoroquinolones with metal ions occurs via the carboxylate and the carbonyl oxygen atoms. It

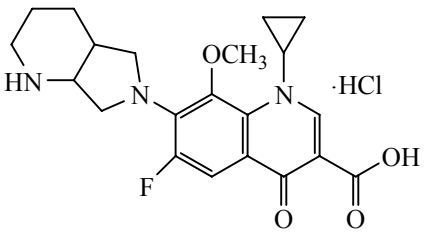

Fig. 1. Structure of moxifloxacin hydrochloride drug (mox-HCl).

[1] The text was submitted by the authors in English.

is less common for piperazine to coordinate via nitrogen atoms [15, 20, 25].

In continuation of our studies of metal-drug complexes [26–30], herein we present synthesis of complexes of moxifloxacin hydrochloride drug with some metal ions (Ca^{II}, Mg^{II}, Zn^{II} and Fe^{III}). The complexes were scrutinized by spectroscopic methods, theoretical calculations, thermal stability assessment, and biological activity.

EXPERIMENTAL

Chemicals and instruments. Moxifloxacin hydrochloride was received from Aldrich chemical company. All chemicals used were analytical grade commercially available from BDH and did not need additional purification.

CHN analysis was carried out in Vario EL Fab. CHNS. The amount of water and the metal percent content were determined by gravimetric analysis. IR spectra of mox-HCl complexes were recorded on Bruker IR spectrophotometer in the range of 400–4000 cm^{-1}. Raman laser spectra of samples were measured on the Bruker FT-Raman with laser 50 mW. The molar conductances of 10^{-3} M solutions of mox-HCl complexes in DMSO were measured on a HACH conductivity meter. All measurements were taken at room temperature for freshly prepared solutions. The electronic spectra of mox-HCl complexes were recorded in DMSO, concentration 1×10^{-3} M, in the range 200–800 nm by Unicam UV–Vis spectrophotometer. The effective magnetic moment (μ_{eff}) of Fe(III) mox-HCl complex was measured at room temperature using Gouy's method by a magnetic susceptibility balance Johnson Metthey and Sherwood [31]. ^{1}H NMR spectra were measured as DMSO solutions on a Bruker 600 MHz spectrometer using TMS as the internal standard. TGA experiments were conducted using Shimadzu TGA-50H thermal analyzers. All experiments were performed using a single loose top loading platinum sample pan under nitrogen atmosphere at a flow rate of 30 mL/min and a 10 deg/min heating rate for the temperature range 25–800°C. SEM images were obtained using a Jeol Jem-1200 EX II Electron microscope at an acceleration voltage of 25 kV. X-ray diffraction (XRD) patterns of the samples were recorded on X Pert Philips X-ray diffractometer. All diffraction patterns were obtained by using Cu$K_{\alpha 1}$ radiation with a graphite monochromator at 0.02 deg/min scanning rate.

Synthesis of complexes. Ca^{II}, Mg^{II}, and Zn^{II} moxifloxacin hydrochloride complexes were prepared by refluxing a mixture of a metal salt and mox-HCl (molar ratio 1 : 2) dissolved in methanol on a hotplate for 3–4 h at ca 65°C. The precipitate formed immediately upon cooling. The corresponding complex of Fe^{III} complex was synthesized according to the same procedure with molar ratio $FeCl_3 \cdot 6H_2O$ to mox-HCl (1 : 3). The colored precipitates were filtered off and washed with methanol and diethyl ether and dried in a vacuum desiccator over $CaCl_2$. Yields of the products were 80–85%.

Antimicrobial assessments. Antimicrobial activity of the complexes was tested using a modified Kirby-Bauer disc diffusion method [32–37]. Briefly, 100 μL of the test bacteria/fungi were grown in 10 mL of fresh media until they reached a count of approximately 108 cells/mL for bacteria or (105 cells/mL) for fungi [33]. 100 μL of microbial suspension was spread onto agar plates corresponding to the broth in which they were maintained. Isolated colonies of each organism that might be playing a pathogenic role should be selected from primary agar plates and tested for susceptibility by the disc diffusion method [34, 35]. Of the many media available, National Committee for Clinical Laboratory Standards (NCCLS) recommends Müller-Hinton agar due to the results good batch-to-batch reproducibility. Disc diffusion method for filamentous fungi was tested by using approved standard method (M38-A) developed by the NCCLS [36] for evaluating the susceptibility of filamentous fungi to antifungal agents and for yeast standard method (M44-P) [37]. Plates inoculated with filamentous fungi as *Aspergillus Flavus* at 25°C for 48 h; Gram (+) bacteria as *Staphylococcus Aureus, Bacillus subtilis*; Gram (–) bacteria as *Escherichia Coli*, *Pseudomonas aeruginosa* were incubated at 35–37°C for 24–48 h and yeast as *Candida Albicans* incubated at 30°C for 24–48 h and then the diameters of the inhabitation zones were measured in millimeters [32]. Standard discs of Tetracycline (Antibacterial agent), Amphotericin B (Antifungal agent) served as positive controls for antimicrobial activity but filter disc impregnated with 10 μL of the solvent (distilled water and DMSO) were used as a negative control. The Meuller-Hinton agar was rigorously tested for composition and pH. This method is well documented and standard zones of inhabitation have been determined for susceptible values. Blank paper disks (Schleicher & Schuell, Spain) with a diameter of 8.0 mm were impregnated

Table 1. Analytical and physical data of mox-HCl drug and their metal complexes

Comp. no.	Color	mp, °C	Λ_m, μs	Elemental analysis, %									
				found					calculated				
				C	H	N	Cl	M	C	H	N	Cl	M
mox-HCl	Yellow	238–242	32	57.34	6.19	9.55	8.06	–	–	–	–	–	–
1	Yellow	>250	34	49.32	5.51	8.19	13.88	2.22	49.89	5.78	8.31	14.03	2.40
2	Yellow	>250	30	49.17	5.41	7.61	13.49	3.76	49.13	5.69	8.18	13.81	3.90
3	Light orange	>250	29	46.99	5.02	10.10	6.42	6.02	47.18	5.09	10.48	6.63	6.12
4	Light brown	>250	38	50.79	5.33	8.40	14.26	3.70	51.06	5.51	8.51	14.35	3.77

Table 2. Characteristic IR/Raman spectra bands and their assignments for the mox-HCl free ligand and its metal complexes **1–4**

mox-HCl	Complex				Assignments
	1	**2**	**3**	**4**	
1704	–	1704	1698	1698	ν(CO); COOH
1620	1574	1620	1618	1622	ν(CO); keto group
–	1620	–	–	–	ν_{as}(COO)
–	1373	–	–	–	ν_{s}(COO)
–	247	–	–	–	$\Delta\nu = [\nu_{as}(COO) - \nu_{s}(COO)]$
–	544, 492	–	–	–	ν(M–O)
–	–	474	461	434	ν(M–N)
–	384, 240	383, 241	–	383, 334	ν(M–Cl); Raman

with 10 μL of the stock solution and placed on agar. The chemical would diffuse from the disc into agar and spread the chemical in agar only around the disc. Zone of inhibition diameters were measured with slipping calipers according to Clinical Laboratory Standers [34]. Agar-based methods such as Etest disk diffusion can be good alternatives because they are simpler and faster than broth methods [38, 39].

RESULTS AND DISCUSSION

Analytical and physical data. Analytical and physical data of the synthesized mox-HCl drug metal complexes are presented in Table 1. The colored solid mox-HCl complexes were stable in the air and insoluble in H_2O and most organic solvents, except for DMSO and DMF upon gentle heating. The products were determined as nonelectrolytes [40]. The structures of mox-HCl complexes were deduced as: $[Mg(mox\text{-}HCl)_2(Cl)_2]\cdot 2H_2O$ (**1**), $[Ca(mox\text{-}HCl)_2(Cl)_2]\cdot 2H_2O$ (**2**), $[Zn(mox\text{-}HCl)_2(NO_3)_2]$ (**3**), and $[Fe(mox\text{-}HCl)_3(Cl)_3]$ (**4**) (see Fig. 2).

The magnetic moment of $[Fe(mox\text{-}HCl)_3(Cl)_3]$ (**4**) complex was measured at room temperature and had paramagnetic character unlike other metals complexes that had diamagnetic nature.

In the IR spectrum of mox-HCl ligand (Table 2) the broad band at 3336 cm^{-1} was assigned to the H-bonded carboxylic group [40–43]. The carboxylic group of mox-HCl molecule demonstrated high frequency of C=O stretching vibration (1704 cm^{-1}) compared to other carbonyl groups of pyridone moiety [42, 43].

Chelation of Ca^{II}, Zn^{II} and Fe^{III} metal ions toward mox-HCl ligand followed two pathways of coordination. First type of coordination: ligation via nitrogen atoms. IR spectra of mox-HCl complexes of Ca^{II}, Zn^{II}, and Fe^{III} were recorded with new bands at 474, 461, and 434 cm^{-1}, respectively, assigned to the ν(M–N) stretching vibrations [42, 43]. The characteristic stretching vibrations of bidentate nitrato group at 1358 and 1028 cm^{-1} were attributed to $\nu_{as}(NO_2)$ and $\nu_{s}(NO_2)$, respectively [42].

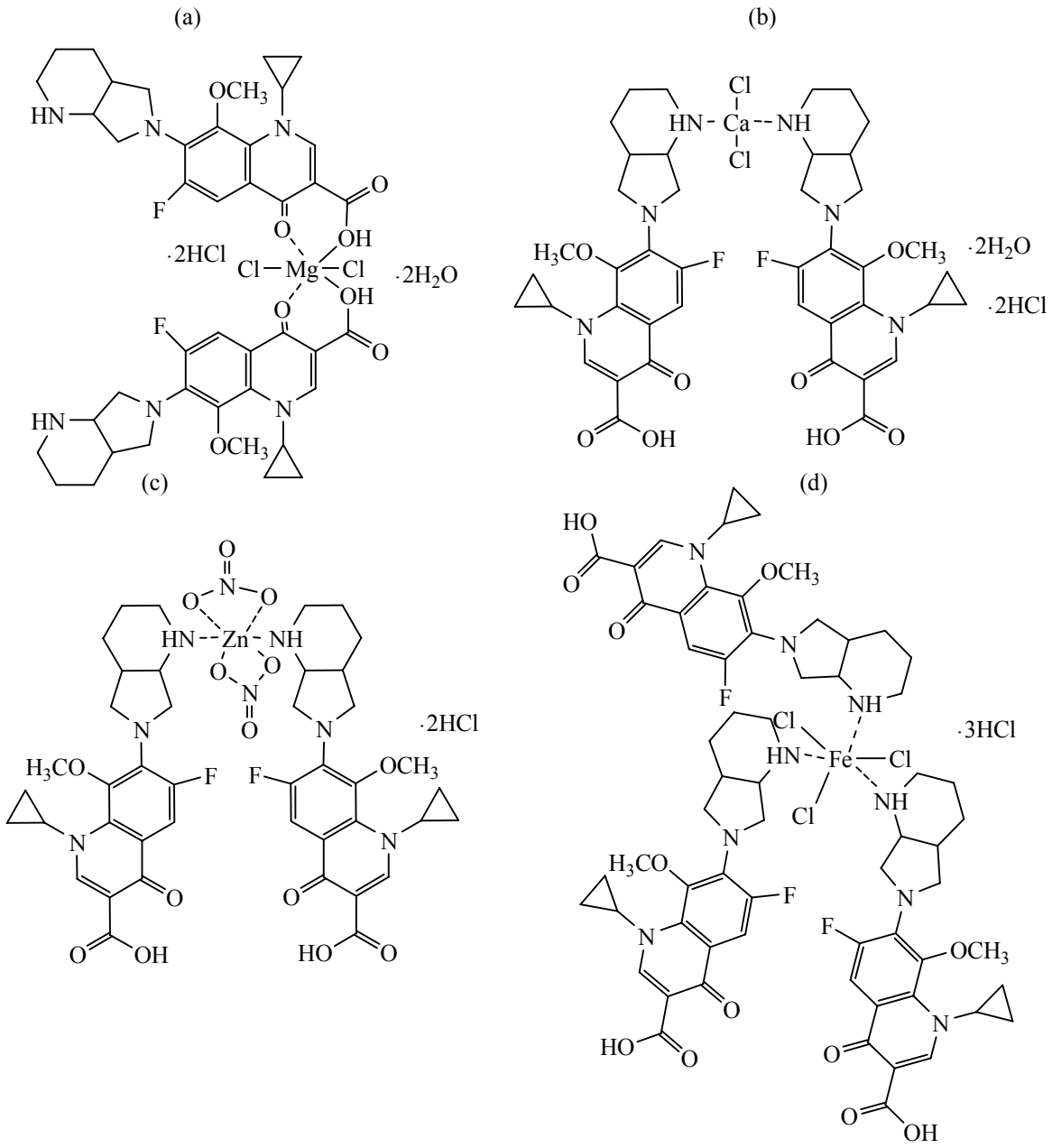

Fig. 2. Suggested structures of (a) $[Mg(mox\text{-}HCl)_2(Cl)_2]\cdot 2H_2O$ (**1**), (b) $[Ca(mox\text{-}HCl)_2(Cl)_2]\cdot 2H_2O$ (**2**), (c) $[Zn(mox\text{-}HCl)_2(NO_3)_2]$ (**3**), and (d) $[Fe(mox\text{-}HCl)_3(Cl)_3]$ (**4**) complexes.

According to the second type of coordination the fluoroquinolones drugs acted as bidentate ligands toward different metal ions via the carboxylate and carbonyl pyridone oxygens to form a stable 6-member ring. In the spectra of Mg(II) complex the band at 1704 cm^{-1} was not recorded due to the formation of a bond between the metal ion and the carboxylate oxygen [42]. Two new bands at 1620 and 1373 cm^{-1} were assigned to asymmetric and symmetric ν(COO), respectively [42]. The difference [$\Delta\nu = \nu_{as}(COO) - \nu_s(COO)$] value of 247 cm^{-1} could be used as an evidence for the bidentate chelation mode of the group [42–45]. IR spectrum of Mg(II) complex demonstrated new bands at 544 and 492 cm^{-1} assigned to the ν(M–O) stretching vibrations [42].

Electronic spectra and magnetic measurements. It is noteworthy that there are no bands assigned to *d–d*

Table 3. UV-Vis spectra and magnetic moments of mox-HCl and its complexes **1–4**

Sample	Electronic bands, λ, nm				μ_{eff}	Geometry
	CT_{M-L}	π–π*	*n*–π*	*d*–*d* transitions		
mox-HCl	280	310, 340	362	–	–	–
Mg(II)	285	305, 350	365, 390	–	Diamagnetic	Octahedral
Ca(II)	280	340	365, 385	–	Diamagnetic	Square planar
Zn(II)	280	330	365		Diamagnetic	Octahedral
Fe(III)	285	330	395	425	5.30	Octahedral

Table 4. ^{1}H NMR data of free mox-HCl ligand and its Mg(II), Ca(II), and Zn(II) complexes

Assignments	δ, ppm			
	mox-HCl	Mg(II)	Ca(II)	Zn(II)
1H; NH piperidyl	10.18	10.18	–	–
1H; COOH	8.66	–	8.66	8.67
3H; OCH_3	3.71	3.70	3.70	3.71
1H; pyridone	8.58	8.54	8.55	8.55
4H; methoxy benzene	7.94, 7.66	7.67, 7.64	7.70, 7.66	7.72, 7.68
4H; pyrolo ring	3.83	3.80	3.80	3.80
6H; piperidyl	1.78, 1.72	1.74, 1.70	1.80, 1.70	1.79, 1.72
6H; cyclopropane	1.10, 3.33	1.10, 3.15	1.09, 3.34	1.10, 3.33

transitions in UV–Vis spectra (Table 3) of complexes **1–3** because of their diamagnetic nature.

The $[Fe(mox\text{-}HCl)_3(Cl)_3]$ (**4**) complex demonstrated a high spin with two absorption bands at 395 and 330 nm that reflected $^6A_{1g}\rightarrow{}^4T_{2g}$ and $^6A_{1g}\rightarrow{}^4T_{1g}$ transitions, respectively [46, 47]. The third band at 285 nm was assigned to the charge transfer (M→L and L→M). The observed magnetic moment value 5.30 B.M. indicated the octahedral geometry of the compound **4** [48, 49].

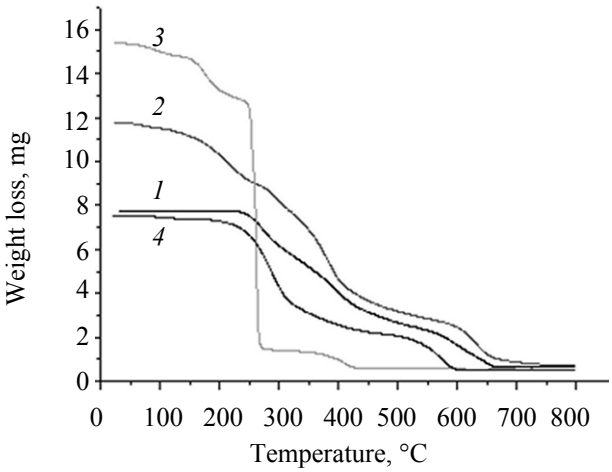

Fig. 3. TG curves of (*1*) $[Mg(mox\text{-}HCl)_2(Cl)_2]\cdot 2H_2O$, (*2*) $[Ca(mox\text{-}HCl)_2(Cl)_2]\cdot 2H_2O$, (*3*) $[Zn(mox\text{-}HCl)_2(NO_3)_2]$, and (*4*) $[Fe(mox\text{-}HCl)_3(Cl)_3]$ complexes.

^{1}H NMR spectra. ^{1}H NMR spectra of Ca(II) and Zn(II) complexes were similar and contained no signals of N–H of the piperidyl ring denoting that the chelation of mox-HCl took place via its piperidyl nitrogen atoms. On the other hand, the presence of proton signals of the carboxylic group excluded its involvement in the coordination. Spectrum of the complex **1** indicated that coordination occurred via the carboxylic group, which was supported by the absence of proton signals of COOH and presence of a signal of N–H (piperidyl ring).

Thermal analysis. Four thermal degradation steps of Mg(II) (**1**) recorded by TG (Fig. 3) with 280, 370, 475, and 580°C maxima corresponded to the loss of $2H_2O$, Cl_2, and 2mox-HCl decomposition. The residual

Table 5. Kinetic data of mox-HCl complexes deduced from the Coats–Redfern equation

Complex no.	Kinetic thermodynamic parameter					r
	E, kJ/mol	A, s^{-1}	ΔS, kJ mol^{-1} K^{-1}	ΔH, kJ/mol	ΔG, kJ/mol	
1	104	1.52×10^2	–206	98	202	0.9983
2	284	4.20×10^2	–200	280	426	0.9911
3	182	2.70×10^2	–206	178	352	0.9986
4	118	1.72×10^2	–204	112	212	0.9992

Table 6. Data of 2θ, intensity, *d*-spacing, crystallite sizes (D), dislocation density (δ), and strain (ε) for complexes **2–4**

Complexes no.	2θ	Intensity	*d*-Spacing	D, nm	$\delta \times 10^{12}$ lin/m^2	$\varepsilon \times 10^{-4}$
2	17.44	3028	5.0809	5.47	0.033	0.118
3	20.20	726	4.3925	2.90	0.119	0.181
4	12.70	1141	6.9646	5.81	0.030	0.144

mass matched with MgO (calculated 3.99%, found 4.60%). The degradation steps of Ca(II) (**2**) TG curve were assigned to the loss of two uncoordinated water molecules and chlorine gas (140 and 330°C). The steps exhibited at DTG_{max} = 498 and 625°C were attributed to the complex decomposed with loss of two mox-HCl molecules. The TG curves for $Zn(mox\text{-}HCl)_2(NO_3)_2$ (**3**) and $Fe(mox\text{-}HCl)_3(Cl)_3$ (**4**) complexes had the similar pattern with three steps (188, 260, and 370°C) and (157, 328, and 532°C), respectively.

Kinetic thermodynamic study. The kinetic thermodynamic parameters of the complexes **1–4** were calculated using the integral method of Coats & Redfern [50] and are presented in Table 5.

The increasing values of ΔG in the mox-HCl complexes were attributed to the structural rigidity of the remaining complex upon expulsion of one and more ligands [51, 52]. Negative values of activation entropies ΔS indicated the more ordered activated complexes than the reactants making the reactions slower [53].

XRD and SEM. X-ray diffraction patterns of Ca(II), Zn(II), and Fe(III) complexes had different reflections with highly crystalline phase contrary to Mg(II) complex which had an amorphous phase. The sharp peaks indicated nano-dimension of the particles. The particle size (D) was calculated from the maximum diffraction patterns [53].

The grain sizes based on Debye–Scherrer formula were calculated to be 5.47, 2.90, and 5.81 nm for the complexes **2–4** respectively [54].

The decrease in the strain and dislocation density indicated the formation of high quality complexes.

Table 7. The quantum chemical parameters of mox-HCl free ligand

Parameters	mox-HCl
Total energy, a.u	–167
Binding energy, a.u	–5.72
Heat formation, a.u	0.951
Electronic energy, a.u	–1131
Dipole moment, B.M.	5.59
E_{HOMO}, eV	–8.4755
E_{LUMO}, eV	0.6525
ΔE, eV	9.1280
χ, eV	3.9115
η, eV	4.5640
σ, eV	0.2191
P_i, eV	–3.9115
S, eV	0.1096
ω, eV	1.6769
ΔN_{max}, eV	0.8570

Table 8. Inhibition zone diameters (mm/mg sample) of mox-HCl and the complexes **1–4** against some kinds of bacteria and fungi

Sample		Inhibition zone diameter (mm / mg sample)					
		B. subtilis (G^+)	*E. coli* (G^-)	*P. aeruginosa* (G^-)	*S. aureus* (G^+)	*A. flavus* (Fungus)	*Candida Albicans* (Fungus)
	Control: DMSO	0.0	0.0	0.0	0.0	0.0	0.0
Standard	Tetracycline Antibacterial agent	34	32	34	30	–	–
Standard	Amphotericin B Antifungal agent	–	–	–	–	18	19
	mox-HCl	30	31	31	40	0.0	0.0
	1	27	28	28	42	0.0	0.0
	2	30	30	28	35	0.0	0.0
	3	31	31	30	41	0.0	0.0
	4	29	27	28	38	0.0	0.0

SEM images demonstrated uniform sizes of particles. The nano-sizes of particles of Ca(II), Zn(II), and Fe(III) complexes **2–4** were very close and dependant upon the aggregation and shape [56].

Molecular modeling. Geometry optimization and conformational analysis for mox-HCl free ligand have been performed using semi-empirical PM3 method implemented in the software of Hyperchem 7.5 program (Table 7).

High value of E_{HOMO} and the increase in global electrophilicity value confirmed that the mox-HCl ligand had a powerful donation ability. The energy gap for the ligand reflected its complexation status.

Antimicrobial assessments. *In vitro* antibacterial and antifungal assessments of the free mox-HCl drug ligand and its complexes **1–4** were assessed against Gram (+) bacteria as *Staphylococcus Aureus, Bacillus subtilis*; Gram (–) bacteria as *Escherichia Coli*, *Pseudomonas aeruginosa* and Fungi as *Candida Albicans* and *Aspergillus flavus*. According to the accumulated data (Table 8) Mg(II) and Zn(II) complexes demonstrated antibacterial activity higher than the free mox-HCl drug against both Gram (+) bacteria (*Staphylococcus Aureus* and *Bacillus subtilis*). The free mox-HCl free drug and its complexes did not display any antifungal activity. Based on the chelation process, the antimicrobial activity status can be interpreted in terms of the overtone's concept of cell permeability and Tweedy's chelation theory [57]. High antimicrobial activity of $[Mg(mox\text{-}HCl)_2(Cl)_2]\cdot 2H_2O$ (**1**) and $[Zn(mox\text{-}HCl)_2(NO_3)_2]$ (**3**) complexes was assigned to their ability of penetration through the lipid membranes and blocking of the metal binding sites in the enzymes of microorganisms. A possible mode of action was determined by reduction of polarity of the metal ions due to partial sharing of a positive charge with the donor groups and possible π-electron delocalization over the whole chelate ring.

ACKNOWLEDGMENTS

This work was funded by Deanship of Scientific Research at university of Taif under project number 3271-435-1.

REFERENCES

1. Zhanel, G.G., Fontaine, S., Adam, H., Schurek, K., Mayer, M., Noreddin, A.M., Gin, A.S., Rubinstein, E., and Hoban, D.J., *Treat. Respir. Med*., 2006, vol. 5(6), p. 437.
2. Blondeau, J.M., Borsos, S., and Hesje, C.K., *J. Chemother*., 2007, vol. 19(2), p. 146.
3. Ming, L.J., *Med. Res. Rev*., 2003, vol. 23(6), p. 697.
4. Žakelj, S., Berginc, K., Uršič, D., and Kristl, L., *Pharmazie*, 2007, vol. 62(4), p. 318.
5. Ming, L.J., *Med. Res. Rev*., 2003, vol. 23, p. 697.
6. Ogunniran, K.O., Tella, A.C., Alensela, M., and Yakubu, M.T., *African J. Biotechnol*., 2007, vol. 10, p. 1202.
7. Sultana, N. and Arayne, M.S., *Pak. J. Pharm. Sci*., 2007, vol. 20, p. 305.
8. Arayne, S., Sultana, N., Haroon, U., and Mesaik, A.M., *Bioinorg. Chem. Appl*., 2009, vol. 2009, p. 1.
9. Cozzarelli, N.R., *Science,* 1980, vol. 207, p. 953.

10. Mitscher, L.A., *Chem. Rev*., 2005, vol. 105, p. 559.
11. Hooper, D.C., *Clin. Infect. Dis*., 2000, vol. 31, p. S24.
12. Maxwell, A., *J. Antimicrob. Chemother*., 1992, vol. 30, p. 409.
13. Ross, D. and Riley, C., *Int. J. Pharmaceut*., 1992, vol. 83, p. 267.
14. Takacs-Novak, K., Noszal, B., Hermecz, I., Kereszturi, G., Podanyi, B., and Szasz, G., *J. Pharm. Sci*., 1990, vol. 79, p. 1023.
15. Refat, M.S., *Spectrochim. Acta, Part A*, 2007, vol. 68, p. 1393.
16. Turel, I., Bukovec, N., and Farkas, E., *Polyhedron*, 1996, vol. 15, p. 269.
17. Ma, H., Chiu, F., and Li, R., *Pharm. Res*., 1997, vol. 14, p. 366.
18. El-Roudi, A.M., Soliman, E.M., and Refaiy, S.A., *Afinidad*, 1989, vol. 420, p. 154.
19. Patel, M.N., Gandhi, D.S., and Parmar, P.A., *Inorg. Chem. Commun*., 2012, vol. 15, p. 248.
20. Gouvea, L.R., Garcia, L.S., Lachter, D.R., Nunes, P.R., de Castro Pereira, F., Silveira-Lacerda, E.P., Louro, S.R.W., Barbeira, P.J.S., and Teixeira, L.R., *Eur. J. Med. Chem*., 2012, vol. 55, p. 67.
21. Vieira, L.M.M., de Almeida, M.V., Lourenço, M.C.S., Bezerra, F.A.F.M., and Fontes, A.P.S., *Eur. J. Med. Chem*., 2009, vol. 44, p. 4107.
22. Drevenšek, P., Košmrlj, J., Giester, G., Skauge, T., Sletten, E., Sepčić, K., and Turel, I., *J. Inorg. Biochem*., 2006, vol. 100, p. 1755.
23. Sultana, N., Arayne, M.S., Rizvi, S.B.S., Haroon, U., and Mesaik, M.A., *Med. Chem. Res*., 2013, vol. 22, p. 1371.
24. Tarushi, A., Polatoglou, E., Kljun, J., Turel, I., Psomas, G., and Kessissoglou, D.P., *Dalton Trans*., 2011, vol. 40, p. 9461.
25. Vieira, L.M.M., de Almeida, M.V., de Abreu, H.A., Duarte, H.A., Grazul, R.M., and Fontes, A.P.S., *Inorg. Chim. Acta*, 2009, vol. 362, p. 2060.
26. Refat, M.S. and Mohamed, S.F., *Spectrochim. Acta, Part A*, 2011, vol. 82, p. 108.
27. Refat, M.S., *J. Mol. Str*., 2013, vol. 1037, p. 170.
28. Refat, M.S., *Spectrochim. Acta, Part A*, 2013, vol. 105, p. 326.
29. El-Megharbel, S.M., Hamza, R.Z., and Refat, M.S., *Spectrochim. Acta, Part A*, 2014, vol. 131, p. 534.
30. El-Megharbel, S.M., Hamza, R.Z., and Refat, M.S., *Chemico-Biological Interactions*, 2014, vol. 220, p. 169.
31. Selwood, P.F., *Magnetochemistry*, New York: Wiley , 1956, 2 ed..
32. Bauer, A.W., Kirby, W.M., Sherris, C., and Turck, M., *Amer. J. Clinical Pathology*, 1966, vol. 45, p. 493.
33. Pfaller, M.A., Burmeister, L., Bartlett, M.A., and Rinaldi, M.G., *J. Clin. Microbiol*., 1988, vol. 26, p. 1437.
34. *National Committee for Clinical Laboratory Standards*, *Performance Volume Antimicrobial Susceptibility of Flavobacteria*, 1997.
35. *National Committee for Clinical Laboratory Standards*. *Methods for Dilution Antimicrobial Susceptibility Tests for Bacteria That Grow Aerobically*, Approved Standard M7-A3, Villanova, Pa, 1993.
36. *National Committee for Clinical Laboratory Standards, Reference Method for Broth Dilution Antifungal Susceptibility Testing of Conidium-Forming Filamentous Fungi*, Proposed Standard M38-A. NCCLS, Wayne, PA, USA, 2002.
37. *National Committee for Clinical Laboratory Standards, Methods for Antifungal Disk Diffusion Susceptibility Testing of Yeast*, Proposed Guideline M44-P, NCCLS, Wayne, PA, USA, 2003.
38. Liebowitz, L.D., Ashbee, H.R., Evans, E.G.V., Chong, Y., Mallatova, N., Zaidi, M., Gibbs, D., et al., *Diagn. Microbiol. Infect*., 2001, Dis. 4, p. 27.
39. Matar, M.J., Ostrosky-Zeichner, L., Paetznick, V.L., Rodriguez, J.R., Chen, E., and Rex, J.H., *Antimicrob. Agents Chemother*., 2003, vol. 47, p. 1647.
40. Soayed, A.A., Refaat, H.M., and Noor El-Din, D.A., *Inorg. Chim. Acta*, 2013, vol. 406, p. 230.
41. Socrates, G., *Infrared Characteristic Group Frequencies*, New York: John Wiley, 1980.
42. Nakamoto, K., *Infrared Spectra of Inorganic and Coordination Compounds*, New York: Wiley, 1970, 2 ed.
43. Bellamy, L.J., *The Infrared Spectra of Complex Molecules*, London: Chapman and Hall, 1975.
44. Deacon, G.B. and Phillips, R., *J. Coord. Chem. Rev*., 1980, vol. 33, p. 227.
45. Sachan, N., Chandra, P., and Yadav, M., *Int. J. Pharm. Pharm. Sci*., 2012, no. 4, p. 383.
46. Cotton, F.A., Goodgame, D.M.L., and Goodgame, M., *J. Am. Chem. Soc*., 1962, vol. 84, p. 167.
47. Figgis, B.N. , *Introduction to Ligand Fields*, New York: Wiley, 1967, p.285.
48. Gunasekaran, S. and Uthra, D., *Asian J. Chem*., 2008, vol. 20(8), p. 6310.
49. Abdalrazaq, E.A., Buttrus, N.H., and Abd Al-Rahman, A.A., *Asian J. Chem*., 2010, vol. 22(3), p. 2179.
50. Coats, A.W. and Redfern, J.P., *Nature*, 1964, vol. 201, p. 68.
51. Yusuff, K.K.M. and Sreekala, R., *Thermochim. Acta,* 1990, vol. 159, p. 357.
52. Frost, A.A. and Peasron, R.G., *Kinetics and Mechanism*, New York: Wiley, 1961.
53. Cullity, B.D., *Elements of X-ray Diffraction*, Addison-Wesley, 1972, Reading, MA, p. 102.
54. Salavati-Niasari, M., Mohandes, F., Davar, F., Mazaheri, M., Monemzadeh, M., and Yavarinia, N., *Inorg. Chim. Acta*, 2009, vol. 362(10), p. 3691.
55. Velumani, S., Mathew, X., and Sebastian, P.J., *Solar Energy Mater. Solar Cells*, 2003, vol. 76, p. 359.
56. Carotenuto, G. and Nicolais, F., *Materials* 2009, no. 2, p. 1323.
57. Raman, N., Kulandaisamy, A., and Chinnathangavel Thangaraja, *Trans. Metal Chem*., 2004, vol. 29, p. 129.